Chapter 11

HTPB-Polyurethane: A Versatile Fuel Binder for Composite Solid Propellant

Abhay K. Mahanta and Devendra D. Pathak

Additional information is available at the end of the chapter

http://dx.doi.org/10.5772/47995

1. Introduction

One of the most promising applications of polyurethane (PU) polymers is as fuel-*cum*-binder material in composite solid propellant. Since the last two decades, PU filled with oxidizer and metallic fuel is being widely used for rockets propulsion. Ariane boosters, shuttles Apogee motors, Peacekeeper (also called the MX-Missile Experimental) missile, Indian Augmented Satellite Launch Vehicle(ASLV) and Polar Satellite Launch Vehicle (PSLV) boosters are some of the motors that are fuelled by PU propellant. PU composite propellant (PCP) is a heterogeneous mixture of polymeric binder, inorganic oxidizer and metallic fuel as the major ingredients. It can be classified as a highly filled PU system in which the three dimensional elastomeric matrix binds the oxidizer and metallic fuel to form a rubbery material. It imparts necessary mechanical properties to the propellant grain to maintain its structural integrity. A PU propellant grain should have sufficient tensile strength and elongation to withstand various types of stresses experienced during handling and transportation, thermal cycling, sudden pressurization on ignition, and acceleration load during flight of the rocket motor. A tensile strength of approximately 7-8 kgf/cm^2, an elongation of 40-50 % and initial modulus of 40-50 kgf/cm^2 are reasonable for a typical case bonded rocket motor (Manjari et al., 1993). The PU binder accounts to 10-15 % of the composite propellant, and usually consists of three components: (1) a prepolymer (polyol), (2) an isocyanate curator, and (3) a chain extender (butan-1,4-diol) and cross-linking agent (trimethylol propane). The most commonly used polyol in recent time is the Hydroxyl Terminated Polybutadiene (HTPB). This liquid prepolymer has excellent physical properties such as low glass transition temperature, high tensile and tear strength, and good chemical resistance (Eroglu, 1998). The hydrocarbon nature of HTPB (98.6%) along with low viscosity (5000 mPas at 30 °C) and low specific gravity (0.90 g/cm^3), makes it a promising fuel binder for PU propellant. It is capable of taking solid loading up to 86-88% without sacrificing the ease of processibility (Muthiah et al., 1992). In addition, it is also a major reducing agent and

gas producing fuel. It is physically and chemically compatible with the conventional oxidizers and other ingredients at normal storage conditions. As it contains mostly carbon and hydrogen, during combustion, it is decomposed to give large volume of stable molecules like carbon monoxide, carbon dioxide, and water vapours increasing the specific impulse of the rocket motor. Additionally, PU obtained from HTPB offers many advantages over conventional polyether and polyester based urethane systems. Properties exhibited by polyurethanes(PUs) prepared from HTPB include (a) excellent hydrolytic stability, (b) low water absorption, (c) excellent low temperature flexibility, (d) high compatibility with fillers and extenders, and (e) formulation flexibility (Sadeghi et al., 2006). Of late, there is a growing demand of segmented HTPB PUs as these PUs have a unique combination of toughness, durability and flexibility, biocompatibility and biostability that makes them suitable materials for use in a diverse range of biomedical applications (Poussard et al., 2004). HTPB based pervaporation membrane technology is the current wave of innovation. It has introduced a new dimension to PU elastomeric technology.

The polymer chemo-rheology and thermo-oxidative degradation are the two relevant key areas of interest, where in-depth knowledge is essential for the effective performance assessment of PU propellants. Chemo-rhelogy is related with the PU processiblity, whereas thermo-oxidation is related to the stability and combustion performance. The information of change on viscosity during the curing process is critical in modelling the PU flow behaviour. Though extensive works have been carried out on this topic in the last decade (Muthiah et al., 1992, Lakshmi & Athithan, 1999, Singh et al., 2002 & Mahanta et al., 2007), it is still a fascinating research area at present. The thermal decomposition of HTPB has been studied exclusively in inert atmosphere (Panicker & Ninan, 1997). However, thermo-oxidative degradation in air, which is the most relevant in view of combustion of the polymer, has not been studied thoroughly. Additionally, the HTPB prepolymer being the decisive component in HTPB PUs, characterization of this polymer (HTPB) at macro as well as micro levels has been of paramount importance in last decade. Two types of HTPB prepolymer are currently in use: i.e., free radical HTPB and anionic HTPB. The free radical grade HTPB is widely used in composite PU propellants because of its low cost and wide availability. The current chapter is focused on prepolymer characterization, rheology, and oxidative degradation of the polymer and the PU systems.

2. Experimental

2.1. Analytical equipments

NMR measurements: The NMR spectra were recorded on a Bruker 800 MHz NMR spectrometer. The HTPB samples (10 % (w/v) for the ^{1}H NMR and 30 % (w/v) for the $^{13}C\{^{1}H\}$ NMR analysis) were recorded in $CDCl_3$ at room temperature. The ^{1}H NMR acquisition parameters were: spectral width = 16 ppm, acquisition time =2 s, relaxation delay = 1 s, pulse width = 90 °, and number of scans =1000. Similarly, $^{13}C\{^{1}H\}$ NMR spectra were recorded using spectral width = 220 ppm, acquisition time = 2 s, relaxation delay = 10 s, pulse width =

90 °, and number of scans = 300. HMQC spectra of HTPB samples (30 % (w/v) in $CDCl_3$ at room temperature) were recorded on a Bruker 500 MHz with a 5 mm inverse Z-gradient probe. Spectral widths: F2 (^1H)=8000 Hz, F1(^{13}C)=27500 Hz. Time domains : (^1H)=1024 and (^{13}C) =515, acquisition time (^1H) =0.23s, delay (^1H) =2s. In processing, the FID was zero-filled to 32 K data points and the resulting 32 K time domain was Fourier transformed. Additionally, Gaussian apodization was also applied in both ^1H and ^{13}C domains. **Viscosity measurements:** A Brookfield HADV-II+ programmable rotational type viscometer equipped with a motorized stand (helipath stand) was used to perform isothermal viscosity measurement at different temperatures. The temperature was controlled by a thermostatic temperature control bath (Brookfield). The temperature control accuracy was ± 0.5 °C. Polymer samples were sheared at different shear rate (rpm). The spindle used for binder slurry was AB-4, whereas for propellant slurry, T-E was used. For each experiment, data was collected after one complete revolution. For each successive revolution, total 10 readings, each at an interval of one second were recorded at the set rotational speed by using Wingather Software. The average viscosity value was calculated and used for data analysis and modelling. **DSC experiments**: Mettler FP-900 thermal analysis system equipped with FP-85 standard cell and FP90 central processor was used for DSC measurement. The heat flow and temperature calibration of DSC were carried out using pure indium metal as per the procedure recommended by the manufacturer (ΔH = 26.7 J/g, MP = 158.9 °C). All experiments were carried out in an air atmosphere at different heating rates, ranging from 2-15 °C/min. Aluminum sample pans (40 μL) were used for the DSC experiments. Almost constant sample mass of 5 ± 1 mg was used. **Tensile properties**: The tensile stress-strain measurements were performed at room temperature, using samples previously kept at 23±2 °C and relative humidity of 50± 5% for 48 hrs, according to ASTM D 618. Elastomeric test specimens were punched from the cured slab using a die prepared in accordance with ASTM D 412-68. Tensile testing was performed in an Instron Universal Testing Machine (UTM) using dumb-bell shaped specimens of cured PUs as well as propellants. A 100 kg load was applied at a crosshead speed of 50 mm/min. Hardness was measured by a Shore A Durometer as per the standard procedure.

2.2. Synthesis of PUs

2.2.1. Unfilled PUs: PU-I and PU-II

The basic compositions that were studied in the present work are shown in Table 1. The binder system studied consists of PU formed by reacting mixture of alcohols [(HTPB, OH value = 42 mg KOH/g), Butanediol (BDO, OH value = 1232 mg KOH/g) as chain extender and trimethylol propane (TMP, OH value = 1227 mg KOH/g) as cross linking agent] with toluene diisocyanate (TDI, purity > 99 percent and a mixture of 2, 4 and 2, 6-isomers in 80:20 ratio). The BDO and TMP were mixed in a fixed ratio (2:1) and dried under vacuum to reduce the moisture content (< than 0.25%) of the mixture. The mixture thus obtained had the hydroxyl value of 1242 mg of KOH/g.

Polyurethane system	Binder component	Fillers (%)	Hard segment content (% w/w)*
PU-I	HTPB/TDI	---	4.34
PU-II	HTPB/TDI/ (BDO +TMP)	---	7.25/7.34/7.43/7.52/7.61
PU-IIp	HTPB/TDI/ (BDO +TMP)	AP- 68, Al -18,	7.25/7.34/7.43/7.52/7.61

*Hard segment content= $\{[w_{TDI} + w_{BDO+TMP}]/w_{total}\} \times 100, w = weight.$

Table 1. The basic composition of the one step PUs.

The PUs were prepared in bulk by one step procedure. Mixing was carried out in a pilot mixer with facility for circulation of hot/cold water around the mixer jacket. The HTPB and BDO-TMP mixture were taken in the pilot mixer and stirred for 10 minutes. The calculated amount of TDI was added to the mixer, and the contents were stirred for 20 minutes at 40 ± 1 °C. The binder slurry was cast in to a Teflon coated mould and cured at 60 °C for 3 days.

2.2.2. Filled PUs (propellant): PU-IIp

The basic propellant composition that uses 68% ammonium perchlorate (AP) and 18% aluminum (Al) powder was taken up for study. AP (with purity > 99%) was used in bimodal distribution (3:1) having average particle size 280 μm and 49 μm, respectively. Particle size of AP and Al powder (mean diameter = 33.51 μm) were measured by a CILAS Particle Size Analyzer-1180 model. Dioctyl adipate (saponification value = 300 mg KOH/g) was used as a plasticizer. The mixing was carried out in two phases. In the first phase, all the ingredients, except the curing agent, were premixed thoroughly for about 3 h at 38 ± 2 °C. Hot water was circulated through the jacket of the mixer bowl to keep a constant temperature throughout the mixing cycle. A homogeneous test of the slurry was carried out after completion of the premix to confirm the uniform dispersion of AP and Al powder. In the second phase of mixing, a calculated amount of curing agent, *i.e.* toluene diisocyanate (TDI) was added to the premixed slurry, and further mixed for 40 minutes at 40 ±1 °C. The propellant slurry was cast in to the Teflon coated mould and cured at 60 °C for 5 days.

3. Results and discussion

3.1. Prepolymer characterization by high field NMR.

The substrate polymer (HTPB) is the key component that affects the elastomeric properties of PUs. Knowledge on the polymer structure and composition is essential for synthesis of PUs with required properties and understanding the various advantages, the polymer can offer. We have used the high field 1D and 2D NMR techniques for characterization of HTPB prepolymers. Analysis of microstructure and sequence distribution of monomer units can be discerned from the analysis of quantitative $^{1}H/^{13}C$

NMR spectra. Although ^{13}C NMR spectroscopy is good in terms of a wider range of chemical shifts and thus offering less possibility of overlapping peaks, problems associated with questionable assignments occasionally arise from steric-sensitive environments in the carbon skeleton. Additionally, the Nuclear Overhauser Enhancement (NOE) of different types of carbon is usually not equal and the wide spin-lattice relaxation time (t_1) range makes quantitative measurements of carbon signals difficult. A combination of NMR techniques such as ^{1}H, $^{13}C\{^{1}H\}$, $^{13}C\{^{1}H\}$-DEPT (Distortionless Enhancement By Polarization Transfer) and $^{1}H/^{13}C$-HMQC (Hetero-nuclear Multiple Quantum Coherence) permit assignments of all ^{1}H and ^{13}C resonance peaks. To our knowledge, hitherto the actual physical characteristics of the HTPB are not precisely known, particularly its absolute number-average molecular weight ($\bar{M}_n$). In the current work, we have examined the ^{1}H and ^{13}C NMR spectra of HTPB in order to precisely determine its number-average degree of polymerization ($\overline{DP}_n$), and thus, $\bar{M}_n$ of the polymer. A typical $^{13}C\{^{1}H\}$ NMR spectrum (200MHz, $CDCl_3$) of free radical HTPB prepolymer is shown in Fig.1. For convenience, resonances in the spectrum can be divided in to three distinct regions, *i.e.* (a) an olefinic region: δ 113-144, (b) a carbon bearing hydroxyl end group region: δ 56 – 65, and (c) an aliphatic region: δ 24-44. However, due to complex nature of the prepolymer, a complete assignment of all signals was not possible. The, methine and methylene carbons were distinguished by using the DEPT technique. The $^{13}C\{^{1}H\}$-DEPT spectrum of the polymer, recorded in $CDCl_3$, is depicted in Fig.2.

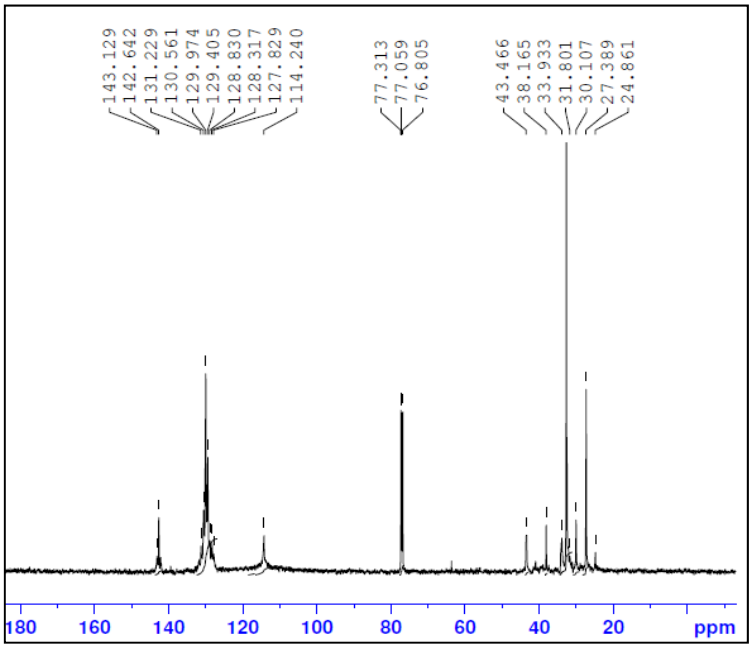

Figure 1. $^{13}C\{^{1}H\}$ NMR ($CDCl_3$, 200 MHz) spectrum of free radical HTPB prepolymer.

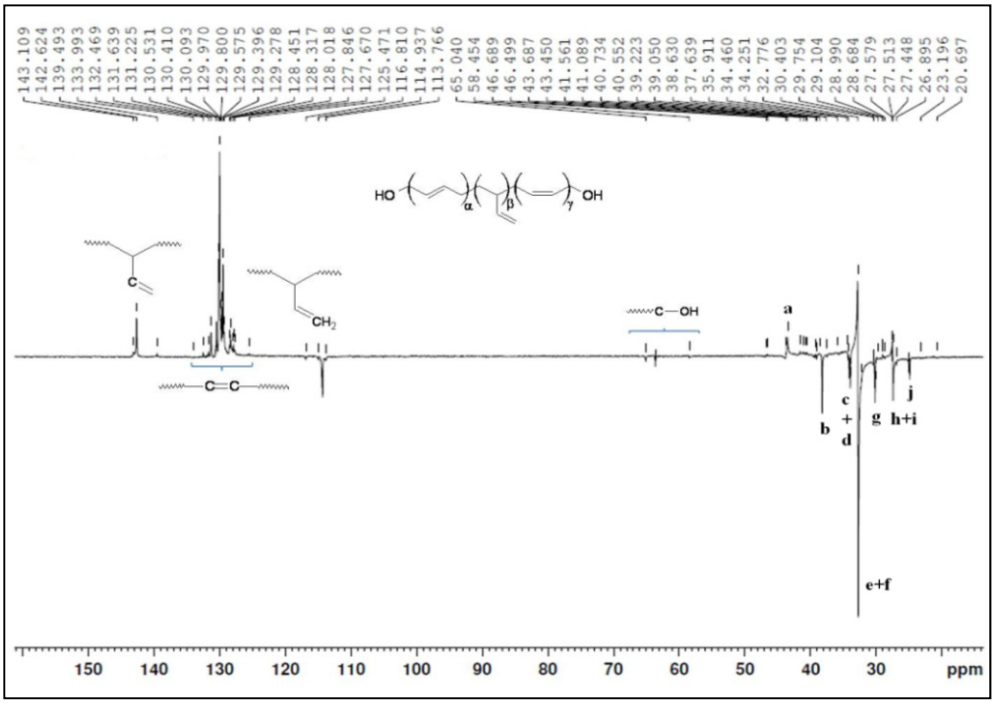

Figure 2. $^{13}C\{^{1}H\}$DEPT-135 spectrum of free radical HTPB prepolymer.

The delay in the DEPT sequence was chosen in such a way that methine carbons appeared as positive peak, whereas both methyl and methylene carbons appeared as negative peak. In the olefinic region, the DEPT spectrum showed a set of positive signals in the range of δ 142-144, that corresponds to methine (-*C*H=) carbons, whereas a set of negative signal at δ 113-115, corresponds to the methylenic (=CH_2) carbons of *vinyl*-1,2- unit. The fine splitting of the signals is due to the tacticity of the monomer units. A set of positive signals in the range of δ 125 – 134 was ascribed to the compositional splitting of the two olefinic carbons (-CH=CH-) in central *cis*-1,4- or *trans*-1,4- unit, present in different combination of homotriads, heterotriads, and symmetric and non-symmetric isolated triads (Frankland et al., 1991). A total of thirteen signals were observed in the olefinic double bond region, *i.e.*δ 127-132. (Fig.3). Each of the resonance line has been assigned to the methine carbon of 1,4-unit in the possible set of three consecutive monomer units (*cis*-1,4-; *trans*-1,4-; and *vinyl*-1,2-unit). When surrounded by 1,2-units, the methine carbon of 1,4-unit would have different chemical shift due to their different distance from the *vinyl*-1,2-side group. The chemical shifts of methine carbon signals in various possible triad sequences were calculated by a known method and then, compared with that of observed one to assign the signals. Besides, the assignment of the triad resonances was made based on the values reported in literature for polybutadiene (Elgert et al., 1975). The results, thus, obtained are summarized in Table 2.

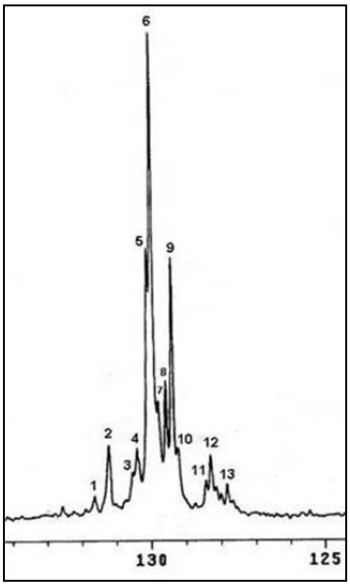

Figure 3. Expanded $^{13}C\{^{1}H\}$ NMR spectrum of δ 127-132 region of free radical HTPB prepolymer.

Signal	Sequence#	Chemical shift (δ values)	
		calculated	observed
1	v-T*-v	131.01	131.6
2	c-T*-v , t-T*-v	130.55	131.2
3	v-C*-v	129.87	130.5
3	v-T*-c ,v-T*-t	129.76	130.4
4	c-T*-c, c-T*-t	129.30	130.1
5	t-T*-c, t-T*-t	129.30	129.9
6	t-*T-v, c-*T-v	129.11	129.8
7	c-*C-c, t-*C-c	128.91	129.4
8	c-*C-t, t-*C-t	128.91	129.3
9	c-*C-v, t-*C-v	128.60	128.8
10	v-*T-t	127.64	128.4
11	v-*T-v	127.45	128.3
12	v-*C-c	127.31	128.0
13	v-*C-t	127.31	127.8

c = *cis*-1, 4-unit; t = *trans*-1, 4-unit; v = *vinyl*-1, 2-unit; v-T*-v = *vinyl*-1, 2-CH_2-CH=CH*-CH_2- *vinyl*-1, 2-unit; and v-*C-t = *vinyl*-1, 2-CH_2-*CH=CH-CH_2- *trans*-1, 4-unit.

Table 2. $^{13}C\{^{1}H\}$ Assignment of triad sequence of free radical HTPB prepolymer (δ 127-132 region).

In the aliphatic region (δ 24-44), the DEPT spectrum showed six sharp negative resonances at δ 38.6, 34.4, 32.8, 30.4, 27.4, and 24.9. A positive signal at δ 43.4, was

assigned to the methine carbon of *vinyl*-1,2- unit. The chemical shift of each aliphatic carbon atom in HTPB polymer can be calculated by using empirical equation for branched and linear alkanes. According to Furukawa, the equation for calculating chemical shift of aliphatic carbon atom is given as $\delta_c(K) = A + \sum_l B_l N_{kl} + C_k$, where $\delta_c(K)$ is the chemical shifts of K carbon, A is a constant, B_l are the parameters away from various positions of K carbon, N_{kl} is the number of carbon away from various positions of K carbon, C_k is the parameter of characteristic structure for K carbon itself. The numerical values of all these parameters were taken from literature (Zheyen et al., 1983). The chemical shifts of the aliphatic carbon atoms in various sequence distribution were calculated and then, compared with the observed one to assign the signals. Besides, the assignment of the diad/triad resonances was made based on the values reported by Sato et al., (1987). The results, thus, obtained are given in Table 3. In the carbon bearing hydroxyl end group region (δ 56-65), the DEPT spectrum showed only the negative resonances (-CH_2-). Therefore, all the resonance signals belong to the adjacent methylene carbon to hydroxyl end group of HTPB prepolymer. Fig.4 shows the expanded $^{13}C\{^1H\}$ NMR spectrum of δ 56-65 region along with the assignment of carbon signals. The assignment of various resonances in this region was based on the report by Haas, (1985). The resonance at δ 58.50 is assigned to methylene carbon of *cis*-1,4-hydroxyl structure while other resonances at δ 63.67 and 65.06 are assigned to the methylene carbon of *trans*-1,4-hydroxyl and *vinyl*-1,2-hydroxyl structure, respectively. Further, the resonance line at δ 56.66 is attributed to the *cis*-1,4-epoxide carbon, while the resonance line at δ 58.26 is assigned to the *trans*-1,4-epoxide carbon.

Signal	Sequence*	Chemical shift (δ values)	
		calculated	observed
a	(1,4)-V-(1,4)	43.10	43.4
b	(1,4)-v-T	35.80	38.6
c	(1,4)-V-v (m)	35.70	34.5
d	(1,4)-V-(1,4)	34.80	34.2
e	T-(1,4) +(1,4)-v-C	33.30-33.40	32.8
f	v-v-C (m)	34.60	32.1
g	T-v/v-V-v	31.0/31.4	30.4
h	(1,4)-C	28.10	27.5
i	C-(1,4)	28.10	27.4
j	C-v	26.40	24.9

*C: *cis*-1, 4-unit; T: *trans*-1, 4-unit; V: *vinyl*-1, 2-unit; (1, 4): C+T; and m: meso.

Table 3. Assignment of $^{13}C\{^1H\}$ NMR resonances of Diad and Triad sequences of free radical HTPB prepolymer (δ 24-44 region).

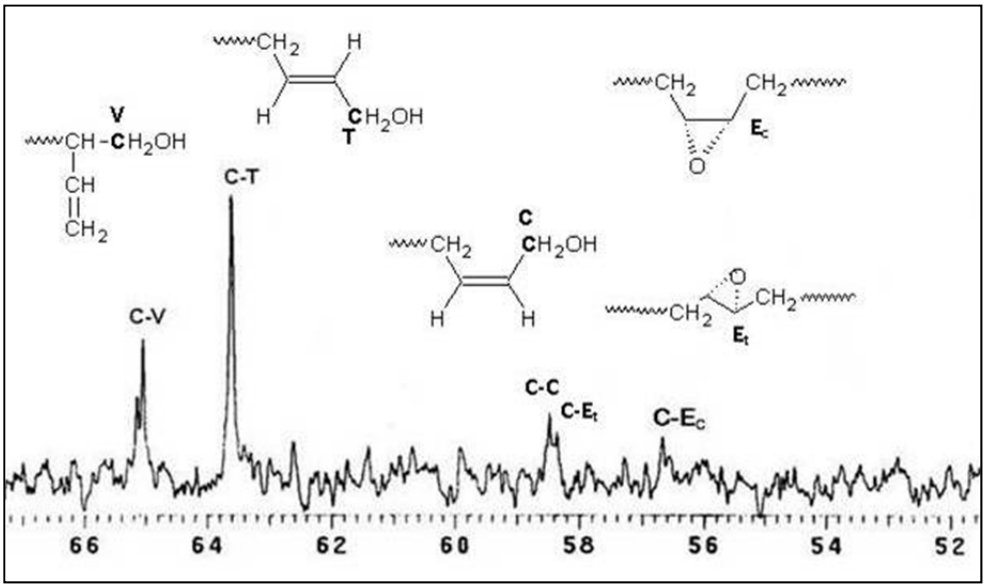

Figure 4. Expanded $^{13}C\{^{1}H\}$ NMR spectrum of δ 56-65 region of HTPB prepolymer along with the assignment of carbon signals.

The assignment of the various methylene and methine carbons from $^{1}H/^{13}C$-HMQC helped to assign the corresponding protons in the ^{1}H NMR spectrum.Figs.5, 6, and 7 show the $^{1}H/^{13}C$-HMQC spectrum of HTPB prepolymer in olefinic region, carbon bearing hydroxyl end group region, and aliphatic region respectively. In the olefinic region, the ^{13}C resonances at δ 113-144, showed three contours in the 2D HMQC spectrum (Fig.5) which corresponded to δ 4.9-5.7, in the ^{1}H NMR spectrum. Further, the fine splitting may be attributed to compositional sequences and tactic reasons. Thus, resonances observed in the HMQC spectrum (Fig.5) at δ 142.8-142.04, 132-127, and 114.9-114.2 corresponded to the protons in the ^{1}H NMR spectrum at δ 5.7-5.4, 5.44-5.41, and 5.0-4.9, respectively. Further, three signals seen in the HMQC spectrum at δ 65.06, 63.67, and 58.5 correspond to the protons at δ 3.4-3.7, 4.1-4.0, and 4.2, respectively (Fig.6). Similarly, in the aliphatic region (Fig.7), the ^{13}C resonance at δ 43.4 and 41.8 is correlated to protons at δ 2.12. The remaining resonances at δ 32.1, 27.4 and 24.9 correspond to the protons at δ 2.10, while the signals at δ 38.6, 32.8 and 30.4 belong to carbons associated with proton signals at δ 2.06. The signals at δ 30.02 and 29.0 are correlated to the protons at δ 1.48 and 1.23 respectively. Based on the above assignments, chemical shifts of various protons observed in the ^{1}H NMR spectrum of the polymer are summarized in Table 4. The proton resonance at 1.23 is assigned to the methyl group of isopropyl ether end group of the polymer. This isopropyl ether end group could be formed as isopropyl alcohol used as solvent in the synthesis of HTPB prepolymer also takes part in the free radical reactions. In presence of hydroxyl radical, isopropoxy radical is formed that leads to the formation of ether terminated polymer (Poletto & Pham, 1994).

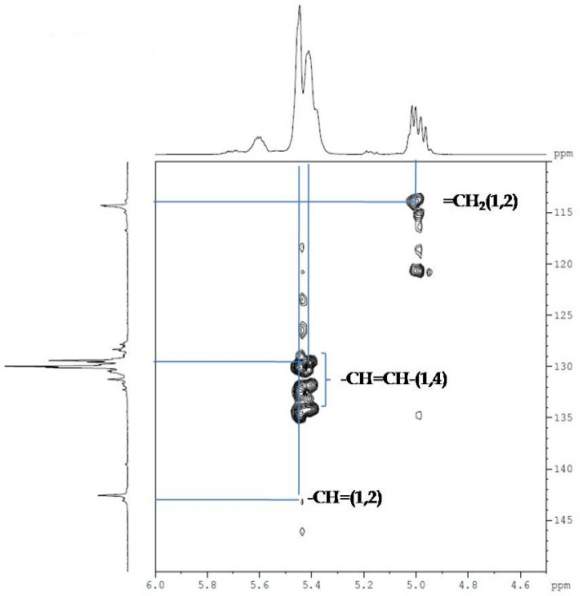

Figure 5. $^{1}H/^{13}C$ HMQC spectra of free radical HTPB prepolymer: olefinic region.

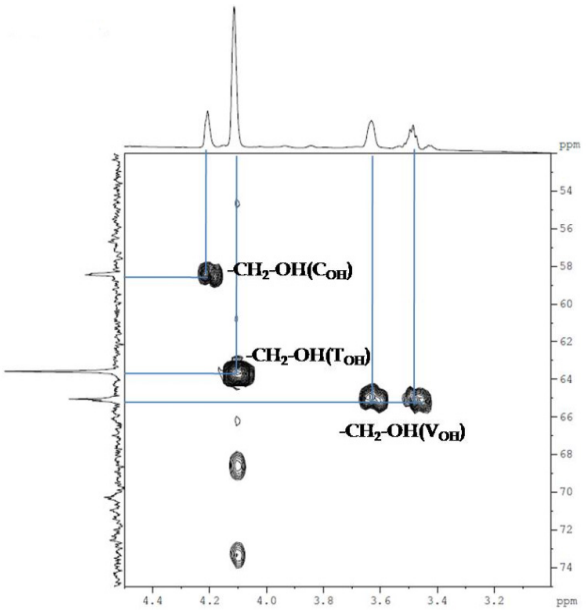

Figure 6. $^{1}H/^{13}C$ HMQC spectra of free radical HTPB prepolymer: carbon bearing hydroxyl end group region.

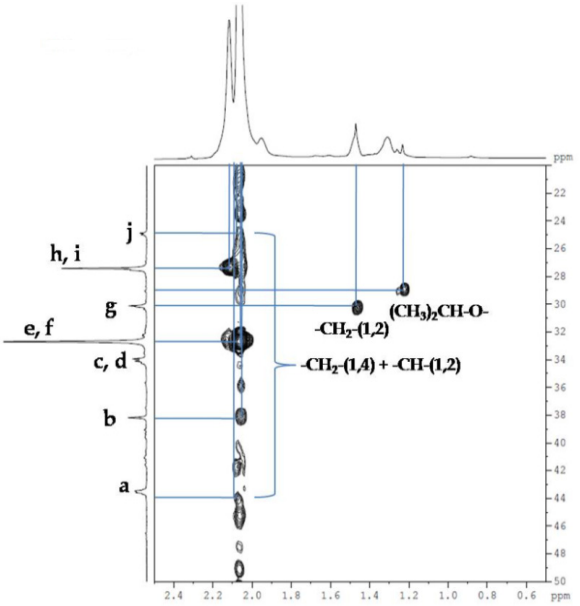

Figure 7. $^{1}H/^{13}C$ HMQC spectra of free radical HTPB prepolymer: aliphatic region.

Hydrogen	Chemical Shifts (δ)
-CH=(1,2) + -CH=CH-(1,4)	5.7-5.4
-CH=CH-(1,4)	5.44-5.41
$=CH_2$-(1,2)	5.0-4.9
$-CH_2$-OH(C_{OH})	4.20-4.16
$-CH_2$-OH(T_{OH})	4.1-4.0
$-CH_2$-OH (V_{OH})	3.7-3.4
$-CH_2$-(1,4) + -CH-(1,2)	2.12-1.90
$-CH_2$-(*cis*-1, 4-unit) + -CH-(1,2)	2.1
$-CH_2$-(*trans*-1, 4-unit)	1.90-2.06
$-CH_2$-(1,2)	1.6-1.3
$(CH_3)_2$CH-O-	1.23

Table 4. Assignments of Chemical shifts (δ) in the ^{1}H NMR spectrum of free radical HTPB prepolymer.

3.1.1. Chain microstructure and relative distribution

The integration of a resonance in NMR is directly proportional to the number of equivalent nuclei contributing to the particular resonance, under suitable experimental conditions. In polymer molecule, these nuclei are part of the chemical structure of a particular repeating unit. Therefore, quantitative result may be obtained by determining the ratio of resonance areas that corresponds to different structural units of the polymer. In Fig.8, the peak

areas corresponding to olefinic (a_1 and a_2) and aliphatic protons (a_3, a_4 and a_5) can be measured separately. Therefore, the mole % of total olefinic protons in HTPB prepolymer can be determined as $olefinic\ protons\ (\%) = (a_1 + a_2)100/(a_1 + a_2 + a_3 + a_4 + a_5)$, where a_1, a_2, a_3, a_4 and a_5 are the integrated areas of peak clusters, as shown the Fig.8. The integrated peak area of a resonance due to the analyte nuclei is directly proportional to its molar concentration and to the number of nuclei that give rise to that resonance. So, we have $a_1 = K_s[2(y + z) + x]$, $a_2 = K_s[2x]$, $a_3 = K_s[4y + x]$, and $a_4 = K_s[4z]$, where K_s is the constant of proportionality. The x, y, and z are the mole fractions of *vinyl*-1,2-; *cis*-1,4-; and *trans*-1,4-content of HTPB, respectively, and $x + y + z = 1$. It can be seen in Fig.8 that each peak cluster is separated from the adjoining one by a sufficient amount of baseline to allow precise measurements. Thus $x, y,$ and z could be calculated by Eqs. (1), (2), and (3), respectively.

$$x = 2a_2/(2a_1 + a_2) \tag{1}$$

$$y = [(2a_3 - a_2)(2a_1 - a_2)]/[(2a_3 - a_2 + 2a_4)(2a_1 + a_2)] \tag{2}$$

$$z = [2a_4(2a_1 - a_2)]/[(2a_3 - a_2 + 2a_4)(2a_1 + a_2)] \tag{3}$$

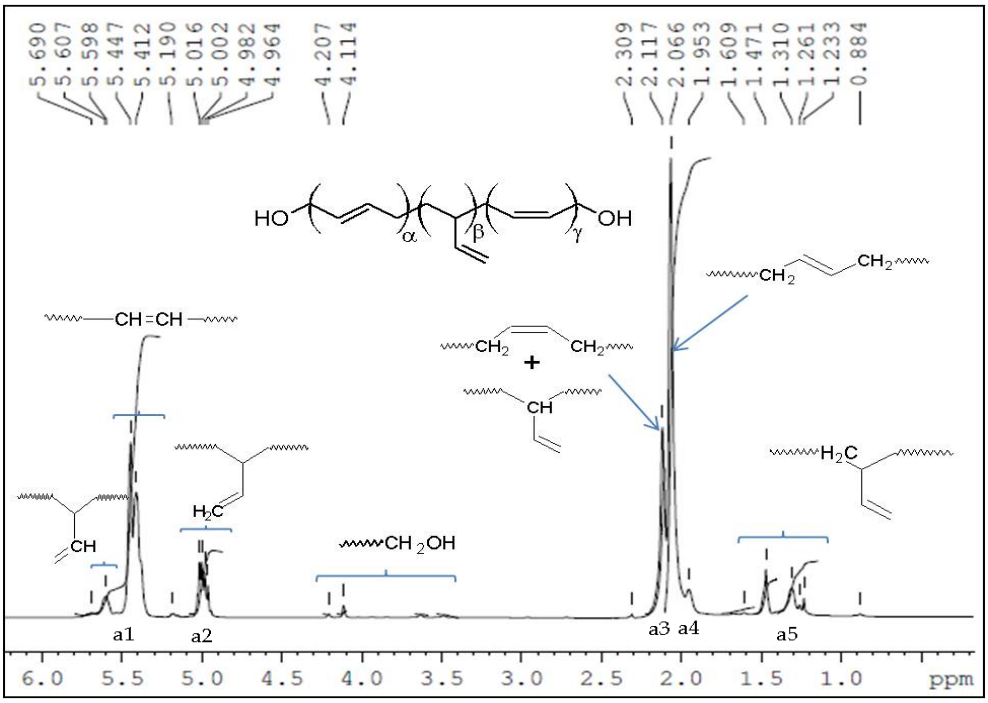

Figure 8. The ^{1}H NMR ($CDCl_3$, 800 MHz) spectrum of free radical HTPB with the assignments of proton signals.

The known microstructures of two commercially available anionic HTPB, *i.e.* Krasol LBH-2000 and LBH-3000 were also examined and the results are given against its standard value for comparison (Table 5). The values given in the parenthesis are the standard value. It clearly shows that the calculated values of the microstructures are very close to that of actual values. This shows the validity of the quantitative FT-NMR (FT-qNMR) method. Following the same procedure, the free radical HTPB prepolymer was analyzed by FT-qNMR method. Table 5 presents the ^{1}H NMR analysis results obtained on backbone microstructure content of the polymer. The microstructures obtained are typical of HTPB prepolymer synthesized by free radical method. Further, HTPB prepolymer has hydroxyl groups attached to the carbon which are in *cis*-, *trans*- or *vinyl*- configuration. Fig.9 shows the expanded ^{1}H NMR spectrum of δ 3.0-4.2 region. This region indicates the resonances of adjacent methylene protons to hydroxyl group of HTPB. Their assignments are shown in Fig.9.

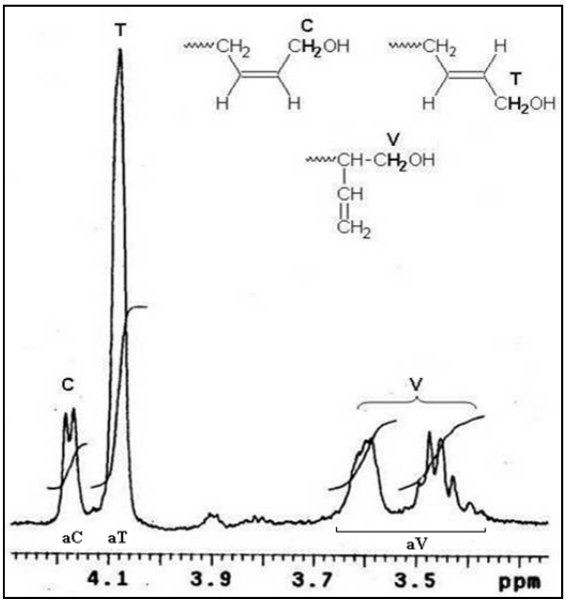

Figure 9. Expanded ^{1}H NMR spectrum of δ 3.0-4.2 region of free radical HTPB prepolymer.

The doublet shown by *cis*-1,4-unit is attributed to the difference in the nature of 1,2- or 1,4-butadiene unit adjacent to it. The complex feature of methylene resonance between δ 3.40 to 3.65 is due to H_A and H_B protons being non-equivalent because of steric hindrance (Fig.10).

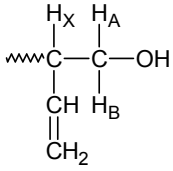

Figure 10. Chemical structure of vinyl-1,2- unit of HTPB prepolymer.

The chemical structure in Fig.10 reveals that all the three protons, *i.e.* H_A, H_B and H_X are magnetically non-equivalent, and therefore, have three different chemical shifts. Further, each of the three signal would split into four peaks (*i.e.* the signal for H_A is split into two by H_B and again into two by H_X proton). The coupling constants between any two of the protons would be different. In fact, two pairs of doublet are observed at δ 3.4-3.5 (H_A) and at δ 3.55 - 3.65 (H_B). The vinylic methine proton (H_X) resonates at δ 2.07. The coupling constant (^3J) between H_A and H_X protons is calculated to be ~8 Hz, where as between H_B and H_X protons is ~6 Hz. The ^2J between H_A and H_B protons is found to be ~18 Hz. The calculated values of coupling constant are in agreement with that of an ABX spin-spin system (Kalsi, 1995). The mole % of *cis*-1,4-; *trans*-1,4-; and *vinyl*-1,2-hydroxyl units were obtained by integrating the corresponding resonances as shown in Fig.9, *i.e.* adding together the integrated amounts and dividing the total into the integrated peak area obtained for each configuration and listed in Table 5. However, in case of Krasol LBH-2000 and LBH-3000 only single broad peak was obtained at δ 3.8.This peak is assigned to the secondary proton of the hydroxyl end group.

3.1.2. Determination of degree of polymerization and molecular weight

The molecular weight of the HTPB prepolymer has significant impact on the end-use properties of PUs. Thus, it needs to be estimated with a high degree of accuracy. More often, the absolute molecular weights of the prepolymer are required for higher precision in performance evaluation. Conventional measurement techniques, such as Vapor Pressure Osmometry (VPO) and Gel Permeation Chromatography (GPC) used for determination of molecular weights of the polymer, being the relative methods do have limitations to produce authentic results. The number average-molecular weight of the polymer could be estimated by ^1H qNMR end-group analysis. The area of an absorption peak in the ^1H qNMR spectrum is proportional to the number of equivalent nuclei and these nuclei are part of the chemical structure of a particular repeating unit. Therefore, in case of HTPB prepolymer, the number-average degree of polymerization ($\overline{DP}_n$) would be the ratio of the sum of olefinic protons integrals to that of hydroxylated methylene protons. The chemical structures of HTPB, synthesized by free radical and anionic polymerization method, are depicted in Fig.11, where α, β and γ are the number of *trans*-1,4- ; *vinyl*-1,2-; and *cis*-1,4- micro structural units respectively.

The number-average degree of polymerization ($\overline{DP}_n$) of HTPB prepolymer would be $\overline{DP}_n = \bar{\alpha}_n + \bar{\beta}_n + \bar{\gamma}_n$, and can be determined by Eq. (4).

$$\overline{DP}_n = \bar{\alpha}_n + \bar{\beta}_n + \bar{\gamma}_n = [(a_2 + 2a_1) \times \bar{F}_n(OH)]/[2(a_C + a_T + a_V)] \quad (4)$$

where a_1 , a_2 , a_C, a_T, and a_V are the integrated peak area of the peak clusters as shown in Figs.8 & 9, and $\bar{F}_n(OH)$ is the average functionality of the prepolymer. Thus, number-average molecular weight ($\bar{M}_n$) can be calculated as $\bar{M}_n(NMR) = (\overline{DP}_n \times 54) + (\bar{F}_n(OH) \times 17)$. Similarly, for Krasol LBH-2000 and LBH-3000, it will be $\bar{M}_n(NMR) = (\overline{DP}_n \times 54) + (\bar{F}_n(OH) \times 59)$. Table 5 presents the results obtained on the three polymers under investigation. The $\bar{M}_n(NMR)/\bar{M}_n(GPC)$ average ratio for free radical HTPB is found to be

0.69, which is well compared with the literature value of 0.67 (Kebir et al., 2005), where as for, Krasol LBH-2000 and LBH-3000, it is 1.03 and 1.15, respectively. This deviation may be due to the narrow distribution of Krasol LBH-2000 and LBH-3000 prepolymer. The polydispersity index (PI) obtained by GPC for Krasol LBH-2000 and LBH-3000 are 1.8 and 1.6, respectively.

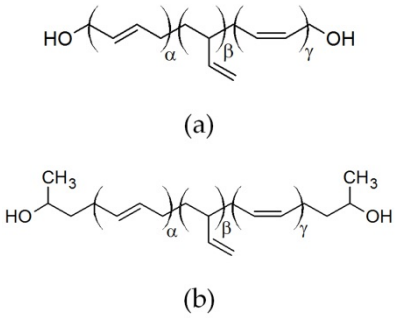

Figure 11. Molecular structure of (a) free radical HTPB, and (b) anionic HTPB prepolymer (Krasol LBH-3000)

HTPB types	Olefinic protons (%)	Microstructure	Hydroxyl types	$\bar{M}_n$		
		C/T/V (%)	C/T/V (%)	NMR	GPC/PI	VPO
LBH-2000	39.96	9.6/21.9/68.4 (12.5/22.5/65.0)	Secondary OH	4208	4068/1.8	2440 (2100)
LBH-3000	40.36	11.4/23.1/65.5 (12.5/22.5/65.0)	Secondary OH	7029	6094/1.6	2630 (3121)
Free radical HTPB	34.50	19.4/59.6/21.0	14.4/57.6/28.0 (Primary OH)	4087	5891/2.1	2590

C: *Cis*-1,4 ; T: *Trans*-1,4 ; and V: *Vinyl*-1,2

Table 5. Results of backbone microstructure, types of hydroxyl end group, and $\bar{M}_n$ of HTPB determined by ^{1}H FT-qNMR method.

3.2. Rheology of HTPB prepolymer: Temperature modelling

The viscosity (μ) of a polymer liquid depends on several variables such as shear rate (γ), molecular weight (M_w), time (t), and temperature (T), *i.e.* $\mu = f(M_w, \gamma, T, t)$. Isothermal viscosity of the prepolymer (HTPB) was obtained at the temperatures of 40 °C, 50 °C, 60 °C, and 70 °C by the Brookfield Viscometer with AB-4 spindle. To check whether shear thinning was occurring, viscosity of the polymer samples was measured at different shear rates (rpm) ranging from 5 to 100 rpm. The samples were also sheared for 10 minutes at a constant shear rate to check the thixotropy nature of the prepolymers. We observed that the viscosity remained more or less same with respect to shear rates indicating a Newtonian characteristic of the prepolymer. Also no effect was observed with time of shearing. Fig.12

shows the effect of temperature on viscosity of the prepolymers (HTPB). The viscosity versus temperature data for Krasol LBH-2000 and LBH-3000 are also included for comparison. It is evident from Fig. 12 that the viscosity decreases with increase in temperature. The temperature dependence of viscosity followed the Arrhenius exponential relation as $\mu(T) = \mu_0 e^{E_{vf}/RT}$, where μ_0=1.32 x10^{-3}, 7.7 x 10^{-7} and 2.11 x10^{-6} mPas and activation energy of viscous flow of the prepolymers E_{vf} = 38.7, 59.23 and 56.54 kJmol^{-1} for free radical HTPB, Krasol LBH-2000 and LBH-3000, respectively (with μ in mPas and T in Kelvin). The viscosity dependence on temperature can also be fitted with a Power Law model of the form $\mu(T) = BT^n$. The Power Law index is the characteristic parameter of the prepolymer. It shows the sensitivity of viscosity to temperature changes ($d\mu/dT$) of the prepolymer. The n values were determined from the log-log plot of viscosity versus temperature (°C) and found to be -2.09, -3.16 and -3.07 for free radical HTPB, Krasol LBH-2000, and LBH-3000, respectively. This indicates that the anionic HTPB prepolymers are more sensitive to the temperature change as compared to the free radical one. Both the Arrhenius and Power Law model satisfactorily described the viscosity dependence on temperature of the polymers as the correlation coefficients were > 0.98.

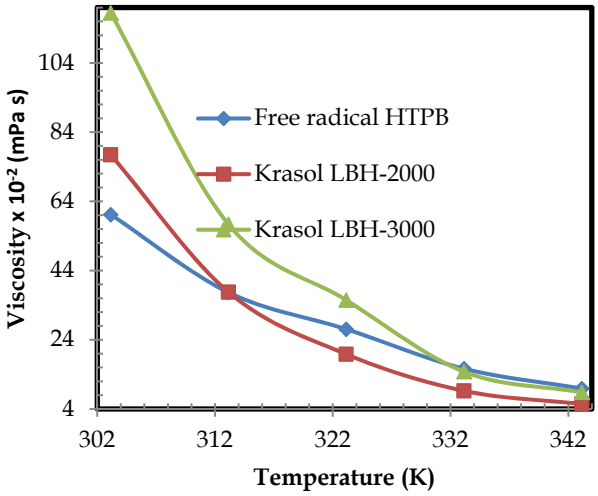

Figure 12. Plots of viscosity(μ) vs. temperature for prepolymers (HTPB).

3.3. Chemo-rheology of PU-I, PU-II and PU-IIp: Temperature and time modelling

Chemo-rheology is the study of chemo-viscosity which is the variation of viscosity caused by chemical reactions. Although the exact reaction mechanism of PU formation is more complex, the kinetics of reaction of diisocyanate with dihydroxyl compound is often expressed successfully by a second order rate equation, *i.e.* $-d[NCO]/dt = k_\mu[NCO][OH]$, where k_μ is the kinetic rate constant. The $[NCO]$and $[OH]$ are the concentration of isocyanate

and hydroxyl groups, respectively. The viscosity of the curing PU system is determined by two factors: (a) the degree of cure, and (b) the temperature. We have carried out the chemo-rheological experiments at different temperatures and different shear rates. As the cure proceeds, the molecular size increases and so does the cross linking density, which in turn, decreases the mobility of the molecules. On the other hand, the temperature exerts direct effects on the dynamics of the reacting molecules and so, on the viscosity. To check whether shear thinning was occurring, viscosity of all the PU samples was measured at different shear rates (rpm) ranging from 5 to 100 rpm (AB-4 spindle) for PU-I and PU-II, whereas for PU-IIp, the shear rate was ranged from 0.5 to 10 rpm (T-E spindle). The samples were also sheared for 10 minutes at a constant shear rate to check the time dependent effect of the PUs. For PU-I and PU-II, we observed that the viscosity remained more or less same with respect to shear rates, which revealed the Newtonian characteristic of the binder resin. Also, no significant effect was observed with time of shearing. However, the PU-IIp (propellant slurry) is found to be shear sensitive. Fig. 13 depicts a typical viscosity build up plots with cure time at various temperatures for PU-I. We observed that viscosity decreased with an increase in temperature. In the initial period of the reaction, when the polymer molecules were small in size, viscosity varied considerably with temperature, higher temperatures resulted in lower viscosities. As the reaction proceeds and molecular size goes up, viscosity rises sharply with respect to time and temperature. This is because the effect of curing reaction overtakes the effect of temperature on viscosity (Reji et al., 1991).

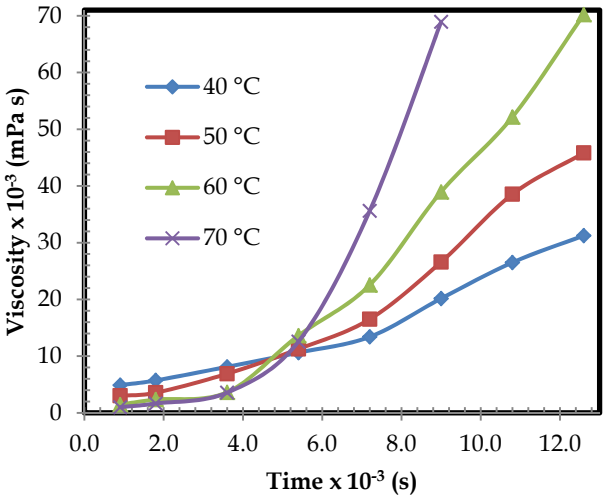

Figure 13. Plots of viscosity (μ) vs. time at various temperatures for PU-1.

The fact that the temperature changes the viscosity of the slurry means that special consideration must be given to kinetic and thermodynamic factors. In kinetics, the emphasis is on the reaction rate. Navarchian et al. (2005) used exponential function to model the viscosity versus time data and found that the semi-logarithmic plots were of good linearity.

The model representing the change of viscosity (μ) with reaction time (t) has the following form:

$$\mu(t) = \mu_0 e^{k_\mu t} \tag{5}$$

where μ_o is the viscosity at t = 0 and k_μ is the rate constant for viscosity build up. This exponential model was applied to the experimental data. The initial viscosity and the rate constants at each temperature were calculated from the intercept and slope of the straight line of $\ln \mu \ vs. t$ plots before the gel point and their values at each isothermal temperature are listed in Table 6.

Temp. (°C)	Unfilled polyurethane				Filled polyurethane	
	PU-I		PU-II		PU-IIp	
	μ_o(mPas)	k_μ(min-1)	μ_o(mPas)	k_μ(min-1)	μ_o (mPas)x10-2	k_μ(min-1)
40	4349	9.76 x 10-3	6320	12.08 x10-3	10869	1.80 x10-3
50	2647	14.62 x10-3	4142	17.70 x10-3	5226	2.80 x10-3
60	1352	20.70 x10-3	2590	27.40 x10-3	3150	4.11 x10-3
70	606	32.49 x10-3	2008	34.80 x10-3	---	---

Table 6. Values of viscosity (μ_o) and rate constants(k_μ) for various PU systems.

The results indicated that the rate constants increased with increase in temperature from 40 to 70 °C, while the μ_o decreased. However, the filled PU (PU-IIp) has shown a very slow build up as it is evident from the very low reaction rate constants. This could be due to the effect of various fillers molecules, which restrict the mobility of the reacting molecules, hence slow down the reaction rate. Further, the relationship of rate constant and viscosity (μ_o) with temperature followed the Arrhenius exponential relationship, *i.e.* $k_\mu(T) = A_\mu \exp(-E_\mu/RT)$, and $\mu_o(T) = A_o \exp(E_o/RT)$, where A_μ and A_o are the apparent rate constant, and initial viscosity at $T = \infty$, E_μ and E_o are the kinetic activation energy, and the viscous flow activation energy, respectively. The values of A_μ, E_μ, A_0, and E_0 of the PU reaction on different systems were determined from the Arrhenius plots and listed in Table 7. Further, unlike unfilled PUs (PU-I and PU-II), the filled PU (PU-IIp) showed the shear thinning behaviour. The effect of shear rate on viscosity is shown in Fig.14. For non-Newtonial material, if the viscosity decreases with shear, the rate of decrease is the measure of pseudoplasticity of the material. The flow of highly loaded propellant slurry (86 % solid loading) can be more closely approximated by the Power Law fluid model (Mahanta et al., 2007). The pseudoplasticity index (PI) and viscosity index were calculated from the curve by fitting to a Power Law equation i.e. $\mu(\gamma) = K\gamma^m$, where μ is the apparent viscosity, γ is the shear rate in rpm, m is the pseudoplasticity index, and K is the viscosity index. Newtonian fluid are the special case of Power Law fluid, when m = 0, viscosity is independent of shear rate. For dilatent fluid m is positive, while for pseudoplastics m varies from 0 and -1. In the current work, for the purpose of characterizing the PU-IIp, the minus sign of the m was excluded and reported in percentage.

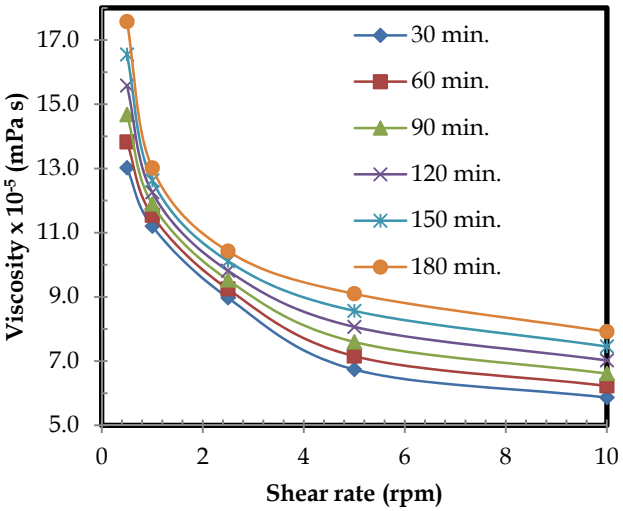

Figure 14. Viscosity (at various intervals) versus shear rate of PU-IIp at 40 °C.

Parameters	Unfilled polyurethane		Filled polyurethane
	PU-I	PU-II	PU-IIp
E_μ(kJ mol^{-1})	35.3	32.3	35.8
E_0(kJ mol^{-1})	58.6	35.0	53.8
A_μ(min^{-1})	7423	3020	1707
A_0(mPas)	7.99 x 10^{-7}	9.03 x 10^{-3}	1.13x10^{-5}
$\Delta S_\mu^\#$ (J mol^{-1} K^{-1})	-180	-187	-192
$\Delta H_\mu^\#$ (kJ mol^{-1})	33.1	29.6	33.1
$\Delta G_\mu^\#$ (kJ mol^{-1}) at 40 °C	89.5	88.3	93.3

Table 7. Kinetic and thermodynamic parameters for different PU-systems.

The pseudoplasticity indexes calculated from the Power Law equation are plotted as a function of cure time (Fig.15).

It is observed that the PI is higher at higher temperature. This indicates that at higher temperature the PU-IIp becomes more non-Newtonian. Interestingly, the PI decreases at 40°C and 60 °C with cure time, whereas at 50 °C, it is almost consistent within the pot life of 3 hours, usually required for casting of the propellant slurry into the rocket case. However, the viscosity index decreased initially with temperature, and afterwards, it increased with the cure time. This is attributed to the increase in cross linking, caused by PU reaction. The flow behaviour of HTPB propellant slurry assumes to have great importance as this is the cause of many grain defects in large scale motor. To make a logical decision regarding propellant mixing and casting, not only the effect of temperature and time on viscosity of

the propellant slurry should be thoroughly studied, but pseudoplasticity of the slurry should also be equally emphasised. This study has indicated that at 50 °C, the PI remains consistent within the required pot life, so it is assumed that propellant mixing and casting at this temperature may result in a better quality grain.

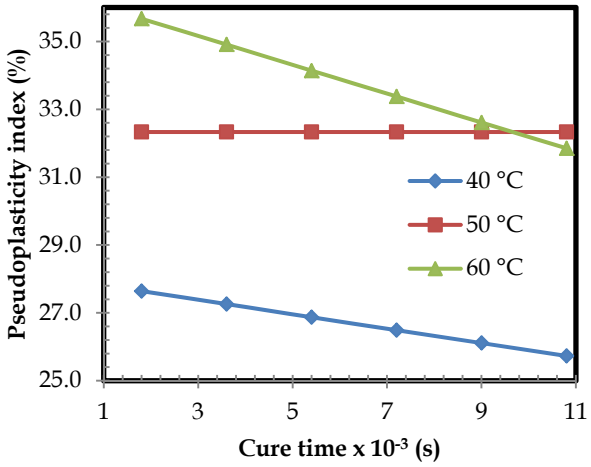

Figure 15. Pseodplasticity index (PI) of PU-IIp as a function of cure time at different temperatures.

A quantitative study of thermodynamic parameters ($\Delta H^{\#}$, $\Delta S^{\#}$, and $\Delta G^{\#}$) helps in understanding the reaction mechanism. It is also used to optimise the cure cycle of the PU reaction, both in terms of time and energy. Wynne-Jones-Eyring–Evans theory (Arlas et al., 2007) presents the temperature dependent pre-exponential factor, and the kinetic constant is given as:

$$k_{\mu} = \frac{k_B T^n}{h} e^{[N+(\Delta S^{\#}/R)]} e^{[-(\Delta H^{\#}+NRT)/RT]} \quad (6)$$

where T is the temperature (K), R = 8.314 Jmol $^{-1}$K^{-1} is the universal gas constant, k_{μ} is the kinetic rate constant, N is called molecularity, h = 6.62 x 10^{-34} Js is the Planck's constant, k_B is the Boltzmann constant, $\Delta H^{\#}$ is the activation enthalpy, and $\Delta S^{\neq}$ is the activation entropy. The classical Arrhenius constant have $N = 0$ and N equals to 1 for reactions occurring in liquid state. Thus, assuming $N = 1$, plotting $\ln(k_{\mu}/T)$ $vs.\, 1/T$, the values of $\Delta H^{\#}$ & $\Delta S^{\#}$ were calculated from the slope and the intercept of the straight line obtained. Also, the $\Delta G^{\#}$ value can be calculated from the fundamental thermodynamic relation, *i.e.* $\Delta G^{\#} = \Delta H^{\#} - T\Delta S^{\#}$. The results thus obtained are listed in Table 7.

It is observed that the activation entropy is negative and quite low. This suggests that the polymerization path is more ordered, that makes the reaction thermodynamically disfavoured. Negative values for activation entropy also indicate the association of reactants prior to chemical reaction.

3.4. Thermo-oxidative degradation of prepolymers (HTPB) and PU-II

The HTPB polymers are vulnerable to oxidative degradation due to it reactive carbon-carbon double bonds and hydroxyl functionality. These prepolymers are exposed to air, humidity, increased temperature and a lot of shear, during processing for PUs manufacturing. Oxygen and water can ingress into the system by several ways during storage, handling as well as processing, leading to oxidative degradation of the polymer. Oxidative degradation is due to reaction with oxygen from air, which can lead to deterioration of the polymer properties. As discussed earlier, the olefinic groups of HTPB may be present in three configurations namely, *cis*-1,4-; *trans*-1,4-; and *vinyl*-1,2-units. The content of these units varies from polymer to polymer. Generally, these olefinic groups are of different reactivity in the oxidation reaction (Duh et al., 2010). As a result, the per centage of *cis*-1,4-; *trans*-1,4-; and *vinyl*-1,2- olefinic groups in the HTPB may have great effect on oxidation rates and product composition. The typical DSC curves obtained for free radical HTPB as well as PU-II are shown in Fig.16. The DSC thermogram of Krasol LBH-3000 is also given for comparison. It is seen that the HTPB prepolymer degrades in two distinct stages, i.e. (1) 170-260 °C, and (2) 290-400 °C when heated up to 400 °C. The first exotherm is attributed to the thermal oxidation reaction of HTPB prepolymer. Upon heating in air atmosphere, HTPB and oxygen are involved in a variety of free-radical reactions as shown in Fig.17. The oxidation reactions, as indicated by the first stage exothermic peak in the DSC thermogram, are attributed to oxygen uptake *via* (a) peroxidation, (b) hydroperoxidation, and (c) crosslinking by peroxide linkage. In the first exotherm, the DSC thermogram of free radical HTPB depicted two peaks, one at 205.0 °C and the other at 244.3 °C, which clearly established that two different oxidative paths ((*i.e.*, peroxidation, and hydroperoxidation) were involved in the oxidation process. In contrary to this, a single peak was observed for Krasol LBH-3000 at 234.5 °C. The plausible explanation for this anomaly could be that the per centage of *vinyl*-1, 2-units in the sample of LBH-3000 was higher as compared to free radical HTPB. Owing to the higher reactivity of *vinyl*-1,2 content, the reaction rate escalates initially resulting in the disappearance of the peak.

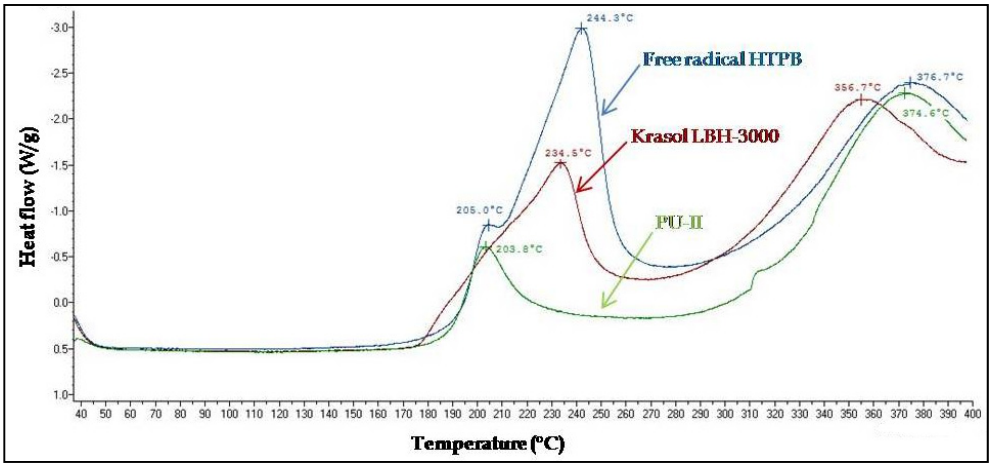

Figure 16. Dynamic DSC scans of HTPB prepolymers and PU-II at the heating rate of 10 °C/min.

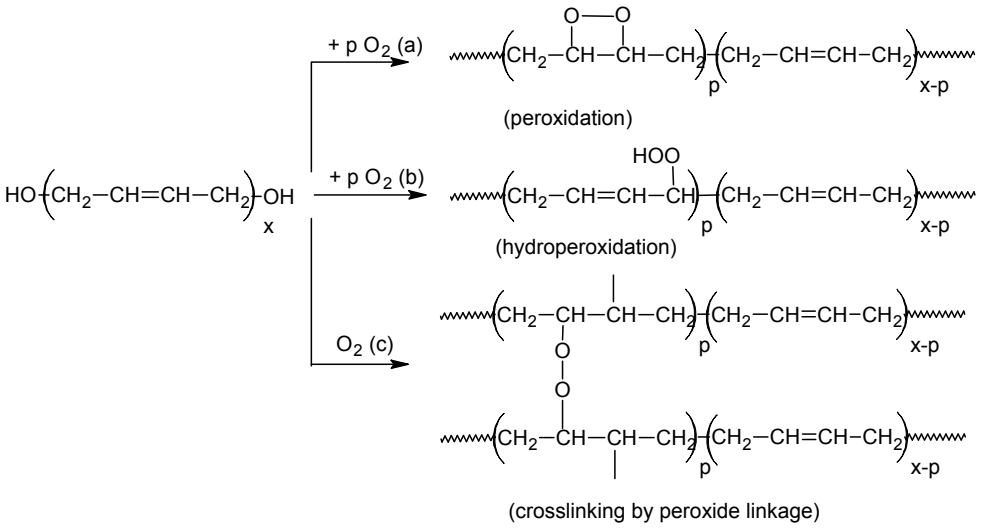

Figure 17. Thermo-oxidative reactions of HTPB prepolymers: (a) peroxidation, (b) hydroperoxidation, and (c) cross-linking by peroxide linkage.

The second exothermic peak occurred at 290-400 °C. The broad exothermic peak is attributed to the major oxidative degradations of HTPB prepolymer involving chain unzipping. It results from the endothermic depolymerisation, exothermic cyclization, and oxidative cross-linking processes of the HTPB prepolymer. The exothermicity is due to the energy released in the formation of new bonds during cross-linking and cyclization, which is greater than the absorbed energy for bond scission during depolymerisation. For PU-II, it is seen that the thermo-oxidative profile has a pattern very similar to that of HTPB prepolymer. This is expected as the PU-II constitutes HTPB more than 92 % of its weight. However, the most important difference is that the thermo-oxidative peak (first exotherm) is slightly less pronounced and occurs somewhat earlier than HTPB prepoymer. The peak temperature of PU-II is 203.8 °C which is 40 °C less as compared to HTPB prepolymer. In second stage i.e. between 290-400 °C, a small elevation is observed around 315 °C, which could be attributed to the cleavage of urethane linkages and subsequent loss of toluene diisocyanate, followed by depolymerization, cyclization, and crosslinking of HTPB prepolymer giving a broad exotherm with peak temperature of 374.6 °C, which is slightly less than its prepolymer peak temperature. This finding is in well agreement with the fact that cleavage of urethane linkages in HTPB PUs is the first step during thermal decomposition (Chen &Brill, 1991). As our objective was to study the thermo-oxidative behaviour of the polymer, we restricted only to the first exothermic peak of the DSC thermogram. The influence of different heating rates (β) on the thermo-oxidative behaviour of free radical HTPB prepolymer is illustrated in Fig.18.The insert in Fig.18 shows the influence of different heating rates (β) on the thermo-oxidative behaviour of PU-II.

We observed from Fig.18 that in both the cases, the thermograms shifted towards higher temperatures as the heating rate (β) increased. This shift of thermograms to higher temperature with increasing heating rate is anticipated since a shorter time is required for the samples to reach a given temperature at a faster heating rate. However, the shapes of the exothermic curves at all heating rates are similar. It indicates that similar reaction mechanisms are involved in oxidative degradation, irrespective of heating rates. The measured values of the onset temperature (T_i), peak temperature (T_p), final temperature (T_f), and oxidation enthalpy (ΔH_{ox}) for HTPB prepolymers and PU-II are listed in Table 8 and 9, respectively.

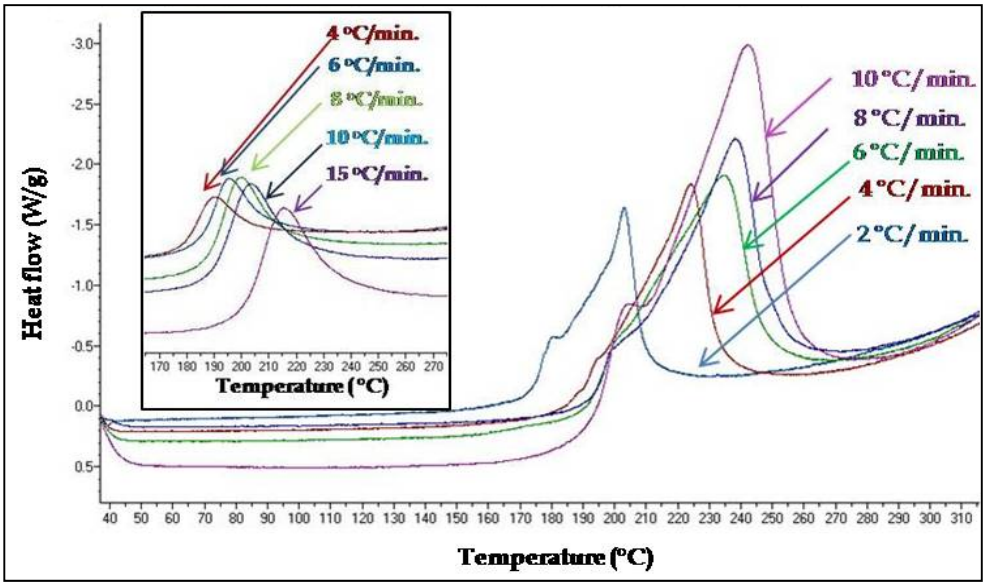

Figure 18. DSC thermogrames for decomposition of free radical HTPB at various heating rates (the insert Fig. is for PU-II).

β (°C min^{-1})	Thermo-oxidative properties of substrate polymers							
	Free radical HTPB				Krasol LBH-3000			
	T_i (°C)	T_p (°C)	T_f (°C)	ΔH_{ox} (Jg^{-1})	T_i (°C)	T_p (°C)	T_f (°C)	ΔH_{ox} (Jg^{-1})
2	159.6	204.1	233.4	896	147.0	188.9	212.4	510
4	177.0	225.4	252.4	653	160.7	206.8	236.1	454
6	186.5	235.7	270.4	595	166.0	216.0	238.9	426
8	187.0	239.1	271.0	649	170.1	222.8	247.1	443
10	187.7	244.3	279.0	628	173.9	234.5	264.4	369

Table 8. Thermo-oxidative properties of HTPB prepolymer at various heating rates (β).

β (°C min^{-1})	Thermo-oxidative properties of PU-II			
	T_i (°C)	T_p (°C)	T_f (°C)	ΔH_{ox} (Jg^{-1})
4	171.4	190.1	216.1	188
6	173.4	195.6	219.3	198
8	175.2	200.4	230.4	134
10	178.7	203.8	233.9	124
15	188.1	215.2	247.7	105

Table 9. Thermo-oxidative properties of PU-II at various heating rates (β).

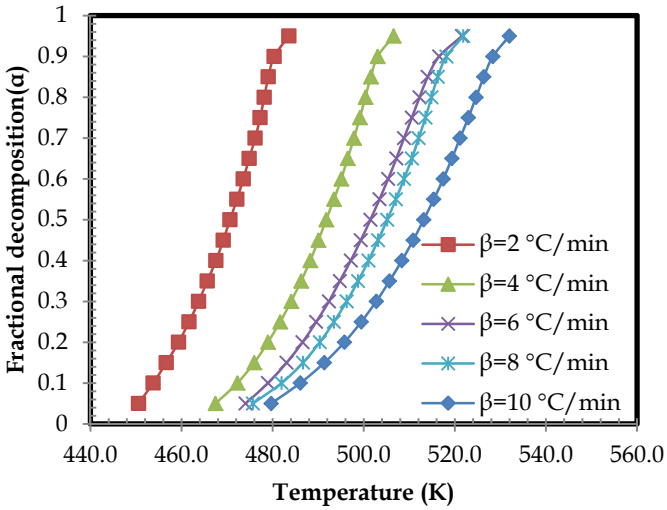

Figure 19. Plots of α versus temperature at different heating rates for free radical HTPB prepolymer.

The fractional decomposition (α) is experimentally determined from the measurement such as heat evolution or mass loss, depending upon the type of experiment performed. In DSC, it is calculated as $\alpha = \Delta H/\Delta H_0$, where ΔH and ΔH_0 are the released heat at certain degree of decomposition and the total heat of decomposition, respectively. Fig.19 shows the variation of fractional conversion as a function of temperature at various heating rates for free radical HTPB. It was seen that the temperature at same conversion increased with the increase of heating rate. A similar trend of conversion change versus temperature was found for PU-II and Krasol LBH-3000 also, under the same range of heating rates.

3.4.1. Kinetics of thermo-oxidation reaction (Model-Free Method)

For a complex reaction like thermo-oxidation reaction with an uncertain reaction mechanism, activation energy is not constant. Therefore, the isoconversional method is the

method of choice for studying the kinetics. The isoconversional methods evaluate the effective activation energy as a function of the extent of conversion. It is assumed that the rate of conversion is proportional to the concentration of reacting molecules. The basic equation used in all kinetics studies is generally described as:

$$\frac{d\alpha}{dt} = k(T)f(\alpha) \tag{7}$$

where, α is the fractional decomposition, $f(\alpha)$ is the single reaction model function, T is the absolute temperature (K), and $k(T)$ is the Arrhenius rate constant. The temperature dependence of the rate constant $k(T)$ is described by Arrhenius equation $k(T) = A\,exp(-E_a/RT)$, where A, R and E_a are the pre-exponential factor, the universal gas constant, and the apparent activation energy, respectively. In non-isothermal conditions, the temperature varies linearly with time. Thus a constant heating rate (β) is defined as $\beta = dT/dt$. Upon introducing the heating rate, $\beta = dT/dt$, Eq.(7) can be modified to

$$\frac{d\alpha}{f(\alpha)} = \frac{\mathrm{A}}{\beta}\exp\left(-\frac{E_a}{RT}\right)dT \tag{8}$$

Therefore, Eq.(8) is the fundamental expression to determine kinetic parameters on the basis of DSC data. In the current work, we have used three different isoconversional methods i.e. (1) Kissinger, (2) Flynn-Wall-Ozawa (FWO), and (3) Kissinger-Akahira-Sunose (KAS) to evaluate the kinetic parameters for thermo-oxidative reaction of the prepolymers (HTPB) and PU-II.

3.4.1.1. Kissinger method

Kissinger (Kissinger, 1956) developed a model-free non isothermal method to evaluate kinetic parameters. In this method, the activation energy is obtained from a plot of $\ln(\beta/T_p^2)$ against $1/T_p$for a series of experiments at different heating rates, where T_p is the peak temperature on the DSC curve.

$$\ln\left(\frac{\beta}{T_p^2}\right) = \ln\left(\frac{AR}{E_a}\right) - \frac{E_a}{RT_p} \tag{9}$$

The activation energy and pre-exponential factor can be calculated from the slope and intercept of the straight line plots of $\ln(\beta/T_p^2)$ versus $1/T_p$.

3.4.1.2. Flynn-Wall-Ozawa method (Flynn &Wall, 1966 and Ozawa,1965)

The integral form of Eq.(8) can be written as

$$g(\alpha) = \frac{\mathrm{A}}{\beta}\int_0^{\mathrm{T}}\exp\left(-\frac{E_a}{RT}\right)dT = \frac{\mathrm{AE_a}}{\beta\mathrm{R}}\,\mathrm{p(x)} \tag{10}$$

where $x = \frac{E_a}{RT}$ and $p(x) = -\int_{\infty}^{\frac{E_a}{Rx}}\frac{\exp(-x)}{x^2}dx$. p(x) is the so-called temperature or exponential integral which cannot be exactly calculated. To describe the thermal degradation kinetics, Ozawa assumed $\ln p(x) \approx -5.330 - 1.052x$ for $20 < x < 60$ for the non-plateau region of the curves, thus Eq. (10) can be written as :

$$\ln g(\alpha) = \ln \frac{AE_a}{\beta R} - 5.330 - 1.052 \frac{E_a}{RT} \quad (11)$$

As A and R are constants, and for a particular conversion, g (α) is constant. Then Eq.(11) becomes

$$\ln \beta = C - 1.052 \frac{E_a}{RT}, \text{where } C = \ln \frac{AE_a}{g(\alpha)R} - 5.330 \quad (12)$$

It is inferred from Eq. (12) that for a constant conversion, a plot of $ln\beta$ versus $1/T$ at different heating rates, should lead to a straight line whose slope provides E_a values. This method is known as Flynn-Wall-Ozawa method (FWO).

3.4.1.3. Kissinger-Akahira-Sunose (KAS) method (Arlas et al., 2007)

In KAS method, the expression p(x) is expressed using the Coats-Redfern approximation. It is $p(x) \cong \frac{\exp[-x]}{x^2}$, substituting this into Eq.(10) and taking logarithms, we get

$$\ln\left(\frac{\beta}{T^2}\right) \cong \ln\left(\frac{AR}{g(\alpha)E_a}\right) - \frac{E_a}{RT} \quad (13)$$

A plot of $ln\,(\beta/T^2)$ versus $1/T$ for a constant conversion gives the E_a at that conversion. We have evaluated the activation energy of prepolymers and PU-II by Kissinger, FWO and KAS methods. The activation energy and pre-exponential factor were calculated from Eq.(9), where T_p is the peak temperature in the DSC curve. The results obtained from Kissinger method are E_a= 68.1, 63.4, 90.6 kJmol^{-1}, $\ln A$ = 14.5, 13.9 and 22.0 min^{-1} for free radical HTPB, LBH-3000 and PU-II respectively. The fact that Kissinger method gives a single value of the E_a and $\ln A$ for the whole process, so it does not reveal the complexity of the reaction. On the other hand, FWO and KAS methods allow evaluating the activation energy at different degree of conversion. For illustration, a typical FWO plots of $ln\beta_i$ versus $1/T_{\alpha i}$ for different values of conversion for free radical HTPB prepolymer are shown in Fig.20. Fig.21 shows the corresponding KAS plots of $ln\left(\beta_i/T_{\alpha i}^2\right)$ versus $1/T_{\alpha i}$ at different values of conversion. Similar plots were obtained for Krasol LBH-3000 and PU-II also, and the $E_a$values were calculated from the slope of the regression lines and are listed in Table 10 and 11. As can be seen that in all the cases, the E_a values obtained from the Kissinger method are well within the range of activation energies ($\alpha = 0.1 - 0.9$) obtained by FWO and KAS methods. We observed that the E_a obtained by FWO method agreed reasonably well to that obtained by KAS method. Moreover, the linear correlation coefficients are all very close to unity. So the results are credible. Additionally, the $E_a$values obtained from FWO method were somewhat higher than the values from the KAS method. This could be due to the approximation techniques used in the integration of the former method.

Further, we observed that E_a decreased with the increase of conversion in both the prepolymer as well as the PU-II. Moreover, the E_a varied with the conversion in a systematic trend, which followed a Power Law function ($E_a = k\alpha^n, r^2 \geq 0.90$). The variation of activation energy with degree of conversion indicates the self-accelerating phenomenon.

In the first step of degradation, the reaction is accelerated once the decomposition starts owing to the decrease of the activation energy at higher conversion. The related hydroperoxidation and peroxidation reaction products are formed with simultaneous loss of un-saturation. The variation of E_a with conversion revealed the existence of a complex multistep mechanism. Moreover, initially the apparent activation energy of the anionic HTPB was marginally higher up to 60% conversion, after that it was same /lower as compared to its free radical counterpart. This reveals that the initiation requires approximately the same activation energy but as the reaction proceeds, the rate of thermo-oxidation is higher for anionic HTPB (Krasol LBH-3000) as compared to free radical HTPB, because of self accelerating effect as anionic HTPB contains the higher per centage of *vinyl*-1,2-units. Also, the activation energy for the PU-II is higher than its prepolymer, which indicates that the PUs are more thermally stable and are less susceptible to oxidation than the substrate polymer. Although, the FWO and KAS methods have advantages in terms of evaluating the activation energy as a function of conversion, the major flaw in the approach is that they do not provide a direct way of evaluating either the pre-exponential factor or the reaction model. On the other hand, model-fitting methods help in fitting different models to α-temperature curves and simultaneously determining the activation energy and pre-exponential factor. There are several non-isothermal model-fitting methods, and the most widely used one is the Coats - Redfern method (Reza et al., 2007).

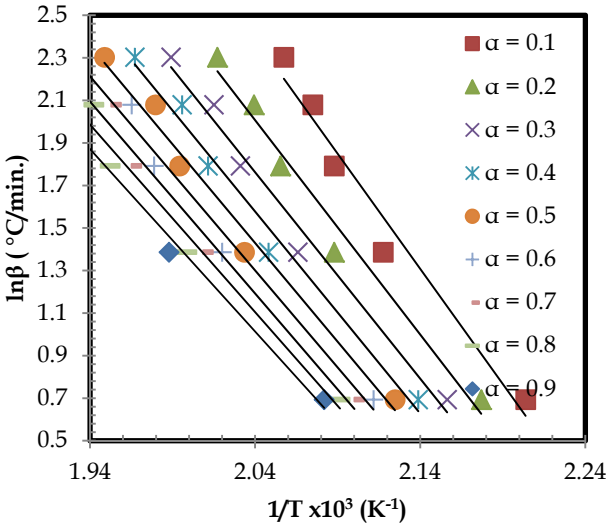

Figure 20. Iso-conversional plots of $ln\beta$ versus $1/T$ (FWO method) for prepolymer (free radical HTPB).

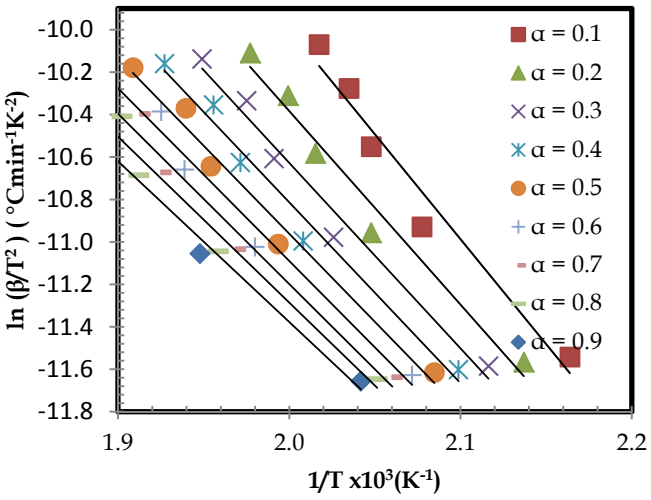

Figure 21. Iso conversional plots of $ln\,(\beta/T^2)$ versus $1/T$ (KAS method) for prepolymer (free radical HTPB).

Conv.	Free radical HTPB				Krasol LBH-3000			
	FWO method		KAS method		FWO method		KAS method	
	ln A * min^{-1}	E_a kJmol^{-1}	ln A * min^{-1}	E_a kJmol^{-1}	ln A * min^{-1}	E_a kJmol^{-1}	ln A * min^{-1}	E_a kJmol^{-1}
0.1	19.4	85.5	18.2	82.2	21.3	88.9	20.2	86.0
0.2	18.0	79.6	16.6	75.8	20.5	86.1	19.4	82.9
0.3	17.2	76.7	15.8	72.7	19.6	82.7	18.4	79.3
0.4	16.8	75.1	15.3	70.9	18.7	79.3	17.3	75.6
0.5	16.4	73.4	14.8	69.0	17.9	76.2	16.4	72.3
0.6	16.1	72.1	14.5	67.7	17.2	73.7	15.7	69.6
0.7	16.0	71.3	14.3	66.7	16.6	71.0	14.9	66.7
0.8	15.6	69.7	13.9	65.0	16.0	68.8	14.3	64.4
0.9	15.3	67.8	13.4	63.0	15.8	67.5	14.0	62.9

Table 10. Kinetic parameters for thermo-oxidative reaction of the prepolymers (HTPB) *(ln A values are calculated assuming the $g(\alpha) = [-\ln(1-\alpha)]^{1/2}$).

Conversion	Polyurethane: PU-II (Free radical HTPB)			
	FWO method		KAS method	
	$\ln A$ *(min^{-1})	E_a ($kJmol^{-1}$)	$\ln A$ *(min^{-1})	E_a ($kJmol^{-1}$)
0.1	24.2	99.0	23.3	96.3
0.2	23.4	96.0	22.5	93.2
0.3	23.0	94.2	22.0	91.3
0.4	22.6	92.6	21.5	89.5
0.5	22.3	91.5	21.2	88.3
0.6	21.9	89.8	20.7	86.5
0.7	21.5	88.4	20.3	85.0
0.8	20.9	86.2	19.7	82.6
0.9	20.2	83.6	18.8	79.8

Table 11. Kinetic parameters for thermo-oxidative reaction of the PU-II *($\ln A$ values are calculated assuming the $g(\alpha) = [-\ln(1-\alpha)]^{1/3}$).

3.4.2. Modelling of thermo-oxidation reaction of prepolymers (HTPB) and PU-II

The activation energies obtained from above three model-free methods (Kissinger, FWO and KAS) could be used to study the possible thermal degradation mechanism of prepolymer and its PU. We have used the Coats-Redfern method (CR) i.e. Eq. (14) to investigate the thermal degradation mechanism of the prepolymers and PU-II.

$$\ln\frac{g(\alpha)}{T^2} = \ln\left[\frac{AR}{\beta E_a}\left(1-\frac{2R\bar{T}}{E_a}\right)\right] - \frac{E_a}{RT} \tag{14}$$

where $\bar{T}$ is the average value of the experimental temperatures. According to CR equation, if a correct model is selected for the thermal decomposition, the plot of $\ln[g(\alpha)/T^2]$ versus $1/T$ will be linear with high correlation coefficient giving the same kinetic parameters as obtained experimentally. First, the probable reaction model was selected and then the parameters were optimised by linear regression to obtain a precise model, which accurately fits the kinetic data. We found that model equation with $g(\alpha) = [-\ln(1-\alpha)]^{1/n}$ (Avrami-Erofeev equation) reasonably fit the kinetic data derived from FWO and KAS method. For prepolymer, n = 2, whereas, for PU-II n = 3. Table 12 lists the kinetic parameters along with the correlation co-efficient calculated by Coats -Redfern method taking $g(\alpha) = [-\ln(1-\alpha)]^{1/n}$ at different heating rates.

On comparison of values of E_a and $\ln A$ calculated by the model equations with those obtained by Kissinger, FWO, and KAS methods, we observed that they were reasonably in good agreement with each other. So, we concluded that the most probable kinetic model function of the thermo-oxidative degradation of prepolymers and PU-II could be described by Avrami-Erofeev equation with $f(\alpha) = 2(1-\alpha)[-\ln(1-\alpha)]^{1/2}$ and $f(\alpha) = 3(1-\alpha)[-\ln(1-\alpha)]^{2/3}$, respectively.

β °Cmin^{-1}	Free radical HTPB			Krasol LBH-3000			Polyurethane: PU-II (Free radical HTPB)		
	$\ln A$ min^{-1}	E_a kJmol^{-1}	r^2	$\ln A$ min^{-1}	E_a kJmol^{-1}	r^2	$\ln A$ min^{-1}	E_a kJmol^{-1}	r^2
2	21.1	91.8	0.994	19.3	82.5	0.997	---	---	---
4	19.4	86.6	0.995	16.3	71.7	0.997	21.0	87.7	0.957
6	16.1	73.7	0.998	15.7	69.0	0.996	22.0	91.0	0.966
8	17.1	77.2	0.995	15.0	66.3	0.996	19.0	79.4	0.955
10	14.4	66.7	0.995	12.4	56.3	0.994	17.9	75.1	0.957

Table 12. Kinetic parameters for no-isothermal oxidation by Coats -Redfern equation.

3.5. HTPB polyurethanes: Stress-strain properties

PU elastomers exhibit good elasticity in a wide range of hard segment contents. This is due to the change of soft or hard segments in different proportion and structure. PUs are composed of short alternating hard and soft segments. The hard segment of PUs usually consists of diisocyanate linked to a low molecular weight chain extender such as butanediol. Meanwhile, the thermodynamic incompatibility between hard and soft segments can lead to the micro-phase separation and hence make a significant contribution to elastomeric properties. Basically, soft segments provide the elasticity, while hard segments play a role in reinforcing the filler and physical cross-linking. In a condensed structure, hard segments usually exist in glassy state or crystalline state. Because of the strong hydrogen bonds of hard segments, their domains can be formed and distributed in the soft segments. The PU elastomeric properties obtained for different systems are reported in Table 13. As a generic trend, it was observed that increase in hard segment content corresponded to higher values of hardness, tensile strength and modulus. The increase in mechanical properties with hard segment content was attributed to the progressive effect of hydrogen bonds within the hard domains of the cross-linked PUs.

Parameters	Unfilled polyurethanes		Filled polyurethanes
	PU-I	PU-II	PU-IIp
Hard segment (% w/w)	4.34	7.25/7.34/7.43/7.52/7.61	7.25/7.34/7.43/7.52/7.61
Elastomeric properties: TS (kgf/cm2)	2.4	3.5/3.6/4.0/4.2/4.4	7.3/8.6/8.9/10.8/11.8
Elong. (%)	350	759/631/627/520/437	44/42/39/35/33
Mod.(kgf/cm2)	---	---	45/52/59/78/83
Hardness (Shore-A)	10	10/14/15/18/20	65/79/80/83/85

Table 13. Elastomric properties of different PU systems.

4. Conclusion

The chapter provides an insight into the microstructure and sequence distribution of the substrate polymer obtained from analysis of 1D and 2D ^{13}C and ^{1}H NMR techniques. The absolute molecular weight of the prepolymer has been determined by high field NMR method. This study pointed out that the HTPB prepolymer was a Newtonian fluid and viscosity decreased exponentially with temperature. The activation energy for viscous flow for free radical HTPB was less than that of anonic prepolymer. The chemo-rheological analysis concludes that the shear rate has no significant effect on the viscosity of the PU reaction within the cure time. The viscosity of various PU systems rises exponentially with cure time. The rate of viscosity build up for filled PU (propellant) is quite low as compared to the unfilled PU systems. Unlike the unfilled PUs, the filled PU slurry showed pseudoplastic behavior, *i.e*. the shear rate had significant effect on viscosity of the propellant slurry. For a typical composition with 86% solid loading, the pseudoplasticity index was found to be higher at higher temperature. It shows that at higher temperature, it becomes more non-Newtonian. Additionally, it also revealed that the pseudoplasticity index remained unchanged within the cure time studied (*i.e.*, 3 h), when maintained at 50 °C, which is desirable in view of propellant flow during casting of the propellant slurry. Further, the filled PU (propellant) gave excellent elastomeric properties, which were apt for solid rocket motor requirement. Additionally, the desired properties can be easily accentuated by simply tailoring the hard segment content of the PU composition. Thermo-oxidative behavior, as studied by DSC of the substrate polymer and the PU elastomers, confirms that PU elastomers are more resistant to thermo-oxidation as compared to the substrate polymer. The thermo-oxidative degradation could be modeled well by an empirical equation given by Avrami-Erofeev. Endowed with so many advantages, HTPB PUs is undoubtedly a versatile and ubiquitous fuel binder for solid rocket motors. However, in order to gain an in depth insight into the multi-step reaction mechanism, further analysis of the DSC data is warranted. Future studies aim at the simulation of the thermo-oxidative profile of HTPB PUs by using a suitable Computer Software in order to understand its complexity.

Author details

Abhay K. Mahanta
Defence Research & Development Organization, SF Complex, Jagdalpur, India

Devendra D. Pathak
Department of Applied Chemistry, Indian School of Mines, Dhanbad, India

Acknowledgement

Authors are thankful to the General Manager SF Complex, Jagdalpur for his kind permission to publish the article.

5. References

Arlas, B.F.; Rueda, L.; Stefani, P.M.; Caba, K.; Mondragon, I. & Eceiza A. (2007). Kinetic and Thermodynamic Studies of the Formation of a Polyurethane Based on 1,6-Hexamethylene Diisocyanate and Poly(carbonate-*co*-ester) Diol. *Thermochimica Acta*, Vol. 459, pp. 94-103

Duh, Y. S.; Ho T.C.; Chen, J.R. & Kao, C. S. (2010). Study on Exothermic Oxidation of Acrylonitrile-butadiene-styrene (ABS) Resin Powder with Application to ABS Processing Safety.*Polymers*, Vol.2, pp. 174-187

Chen, J. K. & Brill, T.B. (1991).Chemistry and Kinetics of Hydroxyl-terminated Polybutadiene(HTPB) and Diisocyanate-HTPB Polymers during Slow Decomposition and Combustion-like Conditions. *Combustion and Flame*, Vol. 87, pp. 217-232

Eroglu, M. S. (1998). Characterization of Network Structure of Hydroxyl Terminated Poly (butadiene) Elastomers Prepared by Different Reactive Systems. *Journal of Applied Polymer Science*, Vol.70, pp. 1129-1135

Elgert, K. F.; Quack, G. & Stutzel, B. (1975). On the Structure of Polybutadiene: 4.^{13}C n. m. r. Spectrum of Polybutadienes with cis-1, 4-, trans-1,4- and 1,2-units. *Polymer*, Vol.16, pp. 154-156

Frankland, J. A.; Edwards, H. G. M.; Johnson, A.F.; Lewis, I.R. & Poshyachinda, S. (1991). Critical Assessment of Vibrational and NMR Spectroscopic Techniques for the Microstructure Determination of Polybutadienes. *Spectrochimica Acta.*, Vol.47A, No. 11, pp.1511-1524

Flynn, J.H. & Wall L. A. (1966).A Quick, Direct Method for the Determination of Activation Energy from Thermogravimetric Data. *Journal of Polymer Science Part B: Polymer Letters*, Vol.4, No. 5, pp. 323-328

Haas, L. W. (1985). Selecting Hydroxy-terminated Polybutadiene for High Strain Propellants. US Patent Number 4536236, pp. 1-8

Kalsi, P. S. (1995). Proton Nuclear Magnetic Resonance Spectroscopy (PMR), *Spectroscopy of Organic Compounds*.2nd ed., pp.165-296, Wiley Eastern Limited, New Delhi

Kebir, N.; Campistron, I.; Laguerre, A.; Pilard, J. F.;Bunel, C.; Couvercelle, J. P. & Gondard, C. (2005). Use of Hydroxytelechelic *cis*-1,4-polyisoprene (HTPI) in the Synthesis of Polyurethanes (PUs). Part 1. Influence of Molecular Weight and Chemical Modification of HTPI on the Mechanical and Thermal Properties of PUs. *Polymer*, Vol.46, pp. 6869-6877

Kissinger, H. E. (1956).Variation of Peak Temperature with Heating Rate in Diffrential Thermal Analysis. *J. of Research of the National Bureau of Standards*,Vol. 57,No.4,pp. 217-221

Lakshmi,R.; & Athithan, S.K. (1999). An Empirical Model for the Viscosity Buildup of Hydroxy Terminated Polybutadiene Based Solid Propellant Slurry. *Polymer Composites* Vol. 20, No.3, pp. 346-356

Manjari, R.; Somasundaran, U. I.; Joseph, V. C. & Sriram, T. (1993). Structure-Property Relationship of HTPB-Based Propellants II. Formulation Tailoring for Better Mechanical Properties. *Journal of Applied Polymer Science*, Vol. 48, pp.279-289

Muthiah, R. M.; Krishnamurthy, V.N. & Gupta B.R. (1992). Rheology of HTPB Propellant.1.Effect of Solid Loading, Oxidizer Particle Size, and Aluminum Content. *Journal of Applied Polymer Science*, Vol. 44, pp. 2043-2052

Mahanta, A. K.; Dharmsaktu, I. & Pattnayak, P.K. (2007). Rheological Behaviour of HTPB-based Composite Propellant: Effect of Temperature and Pot Life on Casting Rate. *Defence Science Journal*, Vol.57, No.4, pp. 435-442

Navarchian, A. H.; Picchioni, F. & Janssen, L. P. B. M. (2005). Rheokinetics and Effect of Shear Rate on the Kinetics of Linear Polyurethane Formation. *Polymer Engineering and Science*, pp. 279-287

Ozawa, T. (1965). A New Method of Analyzing Thermogravimetric Data. *Bulletin of the Chemical Society of Japan*, Vol.38, pp. 1881-1886

Panicker, S. S. & Ninan, K.N. (1997). Influence of Molecular Weight on the Thermal Decomposition of Hydroxyl Terminated Polybutadiene. *Thermochimica Acta* Vol.290, pp. 191-197

Poussard, L; Burel, F.; Couvercelle, J. P.; Merhi, Y.; Tabrizian, M. & Bunel, C. (2004). Hemocompatibility of New Ionic Polyurethanes: Influence of Carboxylic Group Insertion Modes. *Biomaterials*, Vol. 25, pp. 3473-3483

Poletto, S. & Pham, Q. T. (1994).Hydroxytelechelic Polybutadiene, 13[a)] Microstructure, Hydroxyl Functionality and Mechanisms of the radical polymerization of Butadiene by H_2O_2.*Macromol. Chem.Phys.* Vol.195, pp.3901-3913

Reji, J.; Ravindran, P.; Neelakantan, N.R. & Subramanian, N. (1991). Viscometry of Isothermal Urethane Polymerization.*Bull.Chem.Soc.Jpn*.Vol. 64, pp.3153-3155

Reza, E.K.; Hasan A.M. & Ali, S. (2007). Model-Fitting Approach to Kinetic Analysis of Non-Isothermal Oxidation of Molybdenite.*Iran.J.Chem.Chem.Eng*.,Vol.26, No.2, pp.119-123

Sadeghi, G. M. M.; Morshedian J. & Barikani, M. (2006). The Effect of Solvent on the Microstructure, Nature of Hydroxyl End Groups and Kinetics of Polymerization Reaction in Synthesis of Hydroxyl Terminated Polybutadiene. *Reactive & Functional Polymers*, Vol. 66, pp. 255-266

Singh, M.; Kanungo, B.K. & Bansal, T.K. (2002). Kinetic Studies on Curing of Hydroxy-Terminated Polybutadiene Prepolymer-Based Polyurethane Networks. *Journal of Applied Polymer Science*, Vol. 85, pp. 842-846

Sato, H.; Takebayashi, K. & Tanaka, Y. (1987). Analysis of ^{13}C NMR of Polybutadiene by Means of Low Molecular Weight Model Compounds. *Macromolecules*, Vol.20, pp. 2418-2423

Zheyen, Z.; Zinan, Z. & Huimin, M. (1983). ^{13}C-NMR Study on the equibinary (cis-1,4;1,2) Polybutadiene Polymerized with Iron Catalyst. *Polm. Comm.*, No. 1, pp. 92-100